In Vitro and in Vivo Evaluation of a Technetium-99m-Labeled Cyclic RGD Peptide as a Specific Marker of $\alpha_V\beta_3$ Integrin for Tumor Imaging

Zi-Fen Su, Guozheng Liu, Suresh Gupta, Zhihong Zhu, Mary Rusckowski, and Donald J. Hnatowich*

Division of Nuclear Medicine, Department of Radiology, University of Massachusetts Medical School, Worcester, Massachusetts 01655. Received September 20, 2001; Revised Manuscript Received March 11, 2002

Three amino acids residues, Arg-Gly-Asp (RGD), in vitronectin and fibronectin show affinity for $\alpha_V\beta_3$ integrins expressed in vascular endothelial cells. That tumor growth can upregulate the expression of these integrins on tumor cells for invasion and metastasis and in tissue neovasculature suggests the potential of developing radiolabeled RGD peptides as antagonists of $\alpha_V\beta_3$ integrins for broad spectrum tumor specific imaging. The polypeptide RGD-4C, which contains four cysteine residues for cyclization, has shown preferential localization on integrins at sites of tumor angiogenesis. Both RGD-4C and RGE (Arg-Gly-Glu)-4C (as control) were purchased and conjugated with 6-hydrazinopyridine-3-carboxylic acid (HYNIC) for ^{99m}Tc radiolabeling. After purification of the conjugated peptides by a C18 Sep-Pak cartridge with 20% methanol, both peptides were radiolabeled using tricine. For cell binding studies, both ^{99m}Tc peptides were further purified by SE HPLC. High specific radioactivity of labeled cyclized RGD/E (cyclized RGD/E will be simplified as RGD/E through out the text) of about 20 Ci/μmol was achieved. Both ^{99m}Tc complexes were stable in the labeling solution for over 24 h at room temperature. In the human umbilical vein endothelial (HUVE) cell studies, the binding at 1 h of radiolabeled RGD/E was determined at 4 °C and at concentrations in the picomolar to nanomolar range. Under these conditions, cell accumulation of ^{99m}Tc in the case of RGD was as much as 16 times greater than the control RGE. As a check on specificity, 7 nM of native cyclized RGD blocked 50% of the binding of ^{99m}Tc-labeled RGD to cells. The binding percentage of ^{99m}Tc-labeled RGD to purified $\alpha_V\beta_3$ integrin protein, as determined by SE HPLC, increased with the concentration of the integrin while ^{99m}Tc-labeled RGE showed no binding. The association constant for ^{99m}Tc-RGD was modest at 7×10^6 M^{-1}. In both human renal adenocarcinoma (ACHN) and human colon cancer cell line (LS174T) nude mouse tumor models, the accumulation of ^{99m}Tc-labeled RGD/E exhibited no statistical difference. In conclusion, possibly because of limited numbers of $\alpha_V\beta_3$ integrin receptors per tumor cell and low binding affinity, radiolabeled RGD peptides may have limitations as tumor imaging agents.

INTRODUCTION

Tumors must establish a neovasculature to grow. To do so, the endothelial cells need to organize themselves into capillaries anchored to the extravascular matrix. The organization of the vascular endothelial cells is accomplished by an interaction of dimerized single-transmembrane glycoproteins (vitronectin, fibronectin, and von Willebrand factor), named $\alpha_V\beta_3$ integrin, with triplet peptides Arg-Gly-Asp (RGD) sequenced in the proteins of the extracellular matrix (*1*, *2*). The $\alpha_V\beta_3$ integrins are also expressed on cancer cells (*3*, *5*) and therefore play an important role in the invasion (*6*), metastasis (*7*, *8*), proliferation (*9*), and apoptosis of cancer (*10*, *11*). Because the expression of $\alpha_V\beta_3$ integrins is reported to be strong on activated endothelial cells but restricted on normal cells (*12*, *13*), synthetic RGD containing small peptides have been proposed as antagonists (*14*, *15*) against vascular endothelial cell and tumor growth. The RGD peptides, by binding to $\alpha_V\beta_3$ integrin of either endothelial or tumor cells, are capable of inhibiting cell−matrix interaction (*16*), interrupting signal transmission (*17*), affecting cell migration (*18*, *19*), and causing tumor cell regression (*20*, *21*) or apoptosis (*22*, *23*).

The detection of early stage cancer is important in preventing cancer cell metastasis. However, the sensitivity and specificity of current methods for cancer detection especially in early stages are not ideal (*24*). Radiolabeled RGD peptides could be used as a class of tumor (i.e. tumor angiogenesis) specific markers in cancer detection (*25*, *26*). Haubner et al. (*27*) have prepared two ^{125}I-labeled RGD peptides, [^{125}I]-3-iodo-D-Tyr^4-cyclo(-Arg-Gly-Asp-D-Tyr-Val-) and [^{125}I]-3-iodo-D-Tyr^5-cyclo(−Arg-Gly-Asp-D-Phe-Tyr-), as tumor $\alpha_V\beta_3$ integrins antagonists. The accumulation of the ^{125}I-RGD in xenotransplanted melanoma M21 tumors in mice was 1.3−2% ID/g at 1 h postinjection and decreased with time. To improve the tumor uptake, a sugar group was introduced into the cyclic peptides (*28*). The tumor uptake of the glycosylated ^{125}I-RGD remained at 3% ID/g 1 to 4 h postinjection.

It has been reported that the aspartic acid residue of RGD is highly susceptible to chemical degradation leading to the loss of biological activity (*29*). This degradation was prevented when the RGD-containing peptide was cyclized via disulfide linkage (*29*, *30*). In addition to improved stability, these cyclic peptides show higher potency than the linear peptides in inhibiting the attachment of vitronectin (*31*) to cells. Peptide RGD-4C contains four cysteine residues forming two disulfide

* Author for correspondence: Division of Nuclear Medicine, Department of Radiology, University of Massachusetts Medical School, 55 Lake Avenue North, Worcester, MA 01655. Phone: (508) 856-4256; fax: (508) 856-4572; e-mail: donald.hnatowich@umassmed.edu.

10.1021/bc0155566 CCC: $22.00
Published on Web 04/20/2002

linkages in the molecule. In phage display studies, only phage carrying the RGD-4C peptide accumulated in tumor whereas phage carrying another linear RGD peptide did not (*31*, *32*). Preliminary xenotransplanted tumor imaging studies from this laboratory suggested that ^{99m}Tc-labeled cyclic RGD-4C, (Cys^1-Cys^9, Cys^3-Cys^7) H_2N-Cys-Asp-Cys-Arg-Gly-Asp-Cys-Phe-Cys-COOH, may localize on integrins at sites of tumor angiogenesis (unpublished data). However, high specific radioactivity labeling would be required for $\alpha_V\beta_3$ integrin imaging if the number of integrins expressed on tumor vascular cells was low as reported by others (*33*). In this study, we prepared purified ^{99m}Tc-labeled RGD-4C as positive and RGE-4C, (Cys^1-Cys^9, Cys^3-Cys^7)H_2N−Cys-Asp-Cys-Arg-Gly-Glu-Cys-Phe-Cys-COOH, as negative control peptides at high specific radioactivity, carried out an in vitro $\alpha_V\beta_3$ positive human umbilical vein endothelial (HUVE) cell (*34*, *35*) binding test, and imaged the biodistributions of the ^{99m}Tc complexes in nude mice bearing either xenotransplanted human ACHN or LS174T tumors.

EXPERIMENTAL PROCEDURES

Materials and Methods. RGD/E peptides were purchased from Advanced ChemTech (Louisville KY). Succinimidyl 6-hydrazinopyridine-3-carboxylate (NHS−HYNIC) was synthesized as described (*36*). *N*-tris-(hydroxymethyl)methylglycine (tricine), *N*-[2-hydroxylethyl]piperazine-*N*′-[2-ethanesulfonic acid] (HEPES), trifluroacetic acid (TFA), dimethyl sulfoxide (DMSO), and d_6-DMSO were purchased from Aldrich (Milwaukee, WI) or Sigma (St. Louis, MO). Na^{99m}TcO$_4$ was obtained from ^{99}Mo/^{99m}Tc generator (DuPont Pharma, Billerica, MA). C18 Sep-Pak cartridges were produced by Waters Corporation (Milford, MA). The human $\alpha_V\beta_3$ integrin protein (MW 237 kDa, stored in a solution of 20 mM Tris-HCl, pH 7.5, 150 mM NaCl, 2 mM $MgCl_2$, 0.1 mM $CaCl_2$, 0.2% Triton X-100) was obtained from Chemicon International, Inc. (Temecula, CA). Human umbilical vein endothelial (HUVE) cells, endothelial cell basal medium (EBM), and endothelial cell growth medium (EGM) were provided by Clonetics (Walkersville, MD). Human renal adenocarcinoma (ACHN) cell line and human colon cancer cell line (LS174T) were obtained from American Type Culture Collection (Manassas, VA). Minimum essential medium (MEM) and fetal bovine serum (FBS) were purchased from Gibco BRL Products (Gaithersburg, MD). NIH Swiss nude mice were provided by Taconic Labs (Germantown, NY). Nembutal was from Abbott Laboratories (North Chicago, IL).

Zorbax SB300 C18 reversed phase (RP) column (4.6 × 250 mm, 5 μm) was manufactured by Agilent Technologies (Palo Alto, CA). Size exclusion (SE) Superdex Peptide HR 10/30 column (1.0 × 30 cm) was produced by Pharmacia Biotech AB (Uppsala, Sweden). The high performance liquid chromatography (HPLC) system consisted of a 501 and a 510 pump and a 2487 dual channel UV detector (Waters, Milford, MA) fitted with a homemade in-line radiation detector. Radioactive samples were counted in a Packard Cobra II well counter. The centrifuge (Biofuge fresco) was produced by Kendro Laboratory Products (Newtown, CT). Fast-atom-bombardment (FAB-MS) and electrospray ionization (ESI-MS) mass spectra were measured by a JEOL JMS-AX505HA mass spectrometer (JEOL USA, Inc., Peabody, MA).

NHS−HYNIC Conjugation. The RGD/E peptides (1 mg, ∼1 μmol) dissolved in 1 mL of 0.1 M pH 8.0 HEPES buffer were stirred at room temperature. To each solution

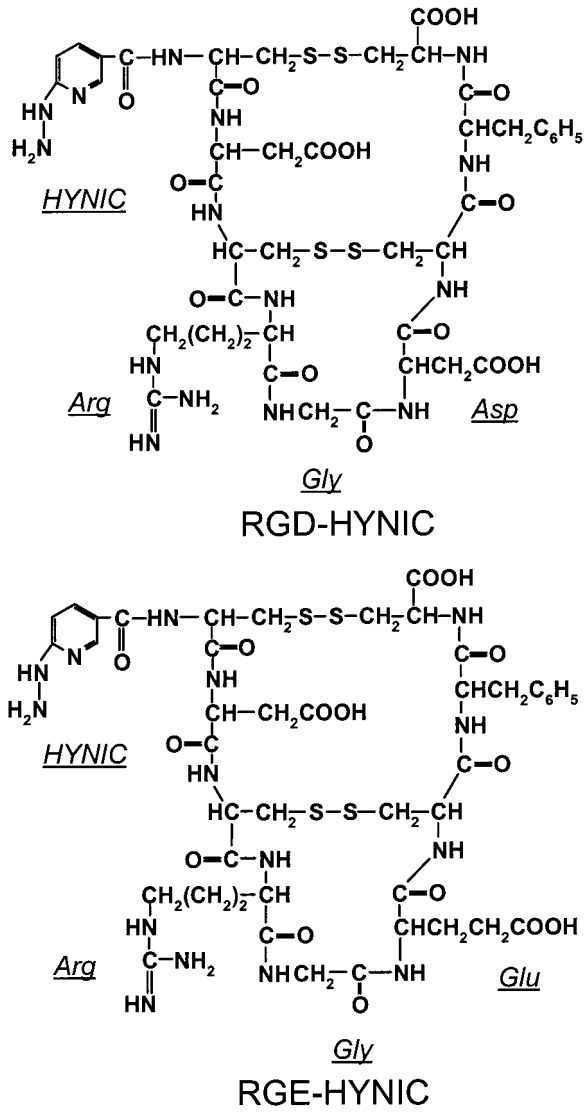

Figure 1. Proposed structures of RGD−HYNIC and RGE−HYNIC.

was added 5 μmol (1.4 mg) of NHS−HYNIC dissolved in 50 μL of dry *N*,*N*-dimethylformamide (DMF, dried over 4 Å molecular sieve). After 1−2 h, the coupling solution was loaded on a C18 Sep-Pak cartridge, preconditioned with 5 mL of methanol followed by 5 mL of water. The loaded cartridge was first washed with 5 mL of water, and 0.3 mL fractions were collected using 20% of MeOH as eluant. Each fraction was analyzed by RP (reversed phase) HPLC with water/acetonitrile solvents pair containing 0.1% TFA as mobile phase with gradient from 100% water to 10% water over 25 min. The fractions with the highest concentration of RGD or RGE, as indicated by UV absorption at 240 and 254 nm, were pooled and lyophilized. Approximately 70% of the theoretical yields were obtained in both cases. The expected structures of RGD/E-HYNIC are shown in Figure 1 and differ only in the extra methylene group of RGE (Glu vs Asp).

Technetium-99m Labeling. The influence of pH values and concentrations of all reagents on the ^{99m}Tc labeling efficiency of RGD/E was investigated. The percentage of pertechnetate and reduced ^{99m}Tc oxide colloid were determined by thin layer and paper chromatography, such as ITLC−SG with saline and Whatman No. 1 paper strip with acetone as developing solvent. The radiochemical purity, recovery, and stability of the ^{99m}Tc-labeled peptides were evaluated by RP HPLC with

either water/acetonitrile or water/acetonitrile containing 0.1% TFA as mobile phase. In this way, labeling conditions were optimized.

The general procedure for ^{99m}Tc labeling of the conjugated peptides was as follows: 0.05 μg to 0.2 μg (0.043−0.17 nmol) of RGD/E-HYNIC in 5 to 20 μL of water, 15 μL of 100 mg/mL tricine in water, 50 μL of 0.25 M pH 5.2 NH_4OAc buffer, 1 to 5 mCi of ^{99m}Tc pertechnetate generator eluant, and 4 to 8 μg of $SnCl_2$ in 10 μL 0.04 N HCl solution were mixed. After incubation at room temperature for 20 min, the labeling solution was analyzed. For in vivo and in vitro tests, the ^{99m}Tc-labeled peptides were purified by SE HPLC collecting every 0.7 mL. The purity of the fraction with the highest radioactivity was tested before use by reanalysis on SE HPLC with 0.1 M pH 7.2 phosphate buffer (PB). The ^{99m}Tc-labeled native RGD/E and NHS−HYNIC were used to identify HPLC peaks due to the radiochemical impurities. Fractions containing the major peaks off RP and SE HPLC for both ^{99m}Tc-labeled peptides were collected separately. The collected fractions were reinjected into both HPLC systems as a check on retention times, radiochemical purity, recovery, and stability.

Binding of Labeled RGD/E to $\alpha_V\beta_3$ Integrin. To establish whether ^{99m}Tc-labeled RGD, like native RGD, shows binding affinity to the $\alpha_V\beta_3$ integrin, both SE HPLC purified labeled RGD and RGE were separately mixed with purified $\alpha_V\beta_3$ integrin protein and analyzed by SE HPLC. Before mixing, the $\alpha_V\beta_3$ integrin protein appeared as a sharp single peak in the UV with retention time of 10.4 min, and the purified ^{99m}Tc complexes of RGD/E appeared in the radioactivity profile as a single peak at 22 min. Purified ^{99m}Tc-RGD ($1.7-2.6 \times 10^{-14}$ mol) along with $2-3 \times 10^{-12}$ mol of unlabeled conjugated RGD and the purified ^{99m}Tc-RGE ($1.9-3.3 \times 10^{-14}$ mol) along with $2-3 \times 10^{-12}$ mol of unlabeled conjugated RGE were mixed with various amounts of the $\alpha_V\beta_3$ integrin protein (5 μg, 10 μg, and 15 μg, $2.1-6.3 \times 10^{-11}$ mol) and analyzed by SE HPLC.

HUVE, ACHN, and LS174T Cells. HUVE cells are known to express $\alpha_V\beta_3$ integrin.[35,37] This cell line was cultured in EGM (500 mL of EBM with supplements of 0.5 mL of 10 ng/mL human recombinant epidermal growth factor (hEGF), 0.5 mL of 1.0 μg/mL of hydrocortisone, and 2.0 mL of a 3 mg/mL solution of bovine brain extract (BBE), 0.5 mL of 50 μg/mL gentamicin, 0.5 mL of 50 ng/mL amphotericin B) containing 10% FBS in a 37 °C incubator with 5% CO_2. The cells were harvested in 0.05% trypsin/0.02% EDTA. After cell counting using a trypan blue dye exclusion assay, the cells were suspended in either EGM, EBM, or PBS at a concentration of 2 to 3×10^6 cells/mL for use. It is assumed that the volume of 500 million HUVE cells is roughly 1 mL.

ACHN and LS174T cell lines were grown in MEM containing 2 mM L-glutamine, 1.5 g/L sodium bicarbonate, 0.1 mM nonessential amino acids, 1.0 mM of sodium pyruvate, 10% FBS, and 100 mg/mL of penicillin−streptomycin. After being harvested and rinsed with trypsin/EDTA, the cells were suspended in MEM with 0.1% human serum albumin (HSA) to a concentration of about 10^7 cells/mL for animal implanting.

Binding of Labeled RGD/E to HUVE Cells. HUVE cells were cultured in EGM containing 10% FBS. After being harvested, the cells were washed in PBS and suspended in either PBS, EBM, or EGM at a concentration of 2 to 3×10^6 cells/mL. To the cell suspension was added 0.01−15 μCi of the SE HPLC purified labeled RGD or RGE. The cell suspension was incubated at 4 °C for 30 min and then centrifuged at 2000 rpm for 4 min. A 30 μL volume of the supernatant was transferred to a plastic tube for radioactivity counting. The cell pellets were washed with cold fresh medium three times and separated from the supernatant for counting. The count (*38*) of the cell pellet was defined as C_{cell}. The count of an equal volume of the supernatant was defined as C_{medium}.

Binding Competition of Labeled RGD and Native RGD to HUVE Cells. Various amounts (final concentration between 50 pM to 58 μM) of native RGD was added to Eppendorf vials containing $2-3 \times 10^6$ HUVE cells suspended in EGM. After incubation at 4 °C for 30 min, the labeled RGD (0.17 μCi) was added, and the cells were incubated for a further 1 h at 4 °C. The vials were centrifuged, and 30 μL of supernatant was transferred for counting. After being washed three times with cold fresh EGM, the cell pellet in the Eppendorf tip was placed in a plastic test tube for counting.

In Vivo Biodistribution of Labeled RGD/E in Tumor-Bearing Mice. LS174T cells (10^6) in MEM containing 0.1% HSA were implanted in one thigh in each of four nude mice. After the tumor grew to approximate 1 cm in any dimension, two animals each received approximately 0.17 μg (0.16 nmol, 24 μCi) of the purified ^{99m}Tc-RGD or RGE. Animals were imaged at 6 h postinjection and were then sacrificed for biodistribution. Radioactivity of the tissue samples was measured against a standard of each injectate.

Each of 10 nude mice was implanted with 10^6 ACHN cells in one thigh. After the tumor size was 1 cm in any dimension, each animal received approximately 4.7 ng (4.1 pmol, 24 μCi) of the purified labeled RGD or RGE. Thus each ACHN-bearing animal received only about 3% of the peptide dosage received by each of the LS174T-bearing animals. The animals were imaged at 6 h postinjection and sacrificed.

Imaging. Mice anesthetized with Nembutal (1.5 mg/25 g mouse) were placed horizontally on the face of the upright collimator. Scintigrams were taken with an Elscint (Hackensack, NJ) APEX 409 M portable large field of view scintillation camera equipped with a parallel hole, medium-energy collimator and an Elscint APEX F1 computer. Images were acquired for a preset time using a 256 × 256 matrix with a 30% energy window set at 140 keV.

RESULTS

HYNIC Conjugation. The molecular mass of RGD measured by FAB-MS was 1017.2714 ($[M + H]^+$, $C_{37}H_{53}N_{12}O_{14}S_4$), calcd 1017.2687, while that of RGE was 1031.2850 ($[M + H]^+$, $C_{38}H_{55}N_{12}O_{14}S_4$), calcd 1031.2843. The errors of the measurements were 2.6 and 0.6 ppm, respectively. The molecular mass of HYNIC-coupled RGD detected by ESI-MS was 1152.3 ($[M + H]^+$, $C_{43}H_{58}N_{15}O_{15}S_4$), calcd 1152.3, whereas the molecular ion of the RGE−HYNIC was not seen on the spectrum. The RGE−HYNIC was then further purified by RP HPLC, lyophilized, and measured by ESI-MS, ES-MS, and FAB-MS, but no expected molecular ion was detected. This may possibly be due to the instability of RGE−HYNIC. C18 Sep-Pak cartridges were used as a simple and effective method to separate the labeled peptides from most of the impurities, such as NHS−HYNIC, hydrated HYNIC, HEPES, and solvents such as DMF. After the purification, the ratio of peptide-HYNIC to uncoupled peptides was in the range of 6 to 10 as indicated by UV absorbance on RP HPLC. Neither native RGD/E exhibited a maximum absorption in the range of 240 nm to 600 nm, while both of the coupled peptides revealed

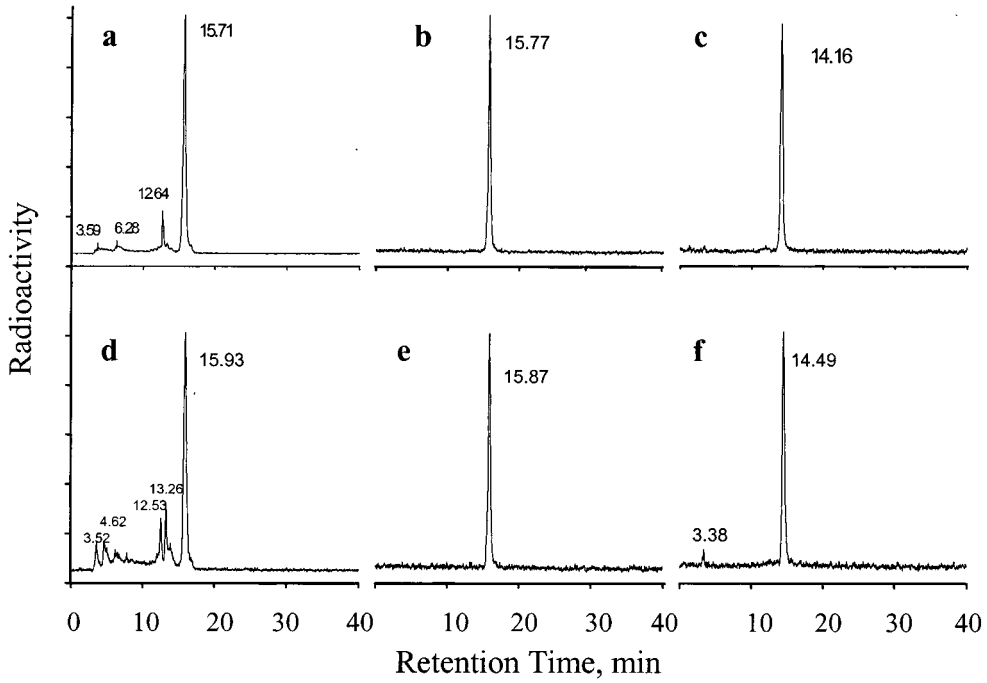

Figure 2. RP HPLC radiochromatograms of ^{99m}Tc-labeled RGD (panel a) and ^{99m}Tc-labeled RGE (panel d) with water/acetonitrile containing 0.1% TFA as mobile phase. The major peak of panels a and d was isolated, re-injected, and analyzed by RP HPLC with (panel b for ^{99m}Tc-RGD and panel e for ^{99m}Tc-RGE) and without 0.1%TFA in the eluant (panel c for ^{99m}Tc-RGD and panel f for ^{99m}Tc-RGE, respectively).

maximum absorption at 283 nm with extinction coefficient of 1.1×10^4 cm^2/mol. The retention times of the native RGD/E on RP HPLC were 15.0 and 15.2 min, respectively. When coupled with HYNIC, the peptides became less hydrophilic than the native peptides and the retention times increased to 15.5 and 15.7 min, respectively. The presence of unlabeled peptides did not significantly affect the ^{99m}Tc labeling of the coupled peptides.

Technetium-99m Labeling. The labeling efficiency of both HYNIC-coupled RGD/E was identical at about 85−90% compared to 10−30% for native, uncoupled RGD/E. Figures 2a and 2d show RP HPLC radiochromatograms (with water/acetonitrile containing 0.1% TFA as mobile phase) of ^{99m}Tc-labeled RGD (retention time 15.7 min) and RGE (15.9 min), respectively. The major peak in Figure 2a was isolated and reinjected into the RP column with (Figure 2b) or without (Figure 2c) 0.1% TFA in the mobile phase. Similarly, the major peak in Figure 2d was isolated and reanalyzed by RP HPLC with (Figure 2e) or without (Figure 2f) 0.1% TFA in the mobile phase. The reanalysis indicated that the purified radiolabeled peptides were pure and stable in the two solvent systems. The ^{99m}Tc labeling of RGD/E without HYNIC produced broad peaks (retention times from 12 to 17 min) on RP HPLC not seen in the labeling of HYNIC coupled RGD/E. Free NHS−HYNIC did not show significant ^{99m}Tc labeling under the same conditions (data not shown). When the labeling was carried out in neutral media, such as water or 0.1 M PB pH 7.2, the impurity peaks at 12.6 to 13.3 min (Figure 2a, 2d) could be as high as 44% but were much lower at 11−22% when the labeling was carried out in 0.25 M acetate buffer pH 5.2. Little pertechnetate remained but approximately 10−15% of ^{99m}Tc was present as radiocolloids. Presumably for this reason, approximately 30−50% of ^{99m}Tc was retained on the RP or SE column during the HPLC purification of the labeled peptides. The formation of radiocolloids could be reduced through the use of ^{99m}Tc-gluconate or ^{99m}Tc-tartrate as transfer ligands, but the labeling efficiency then decreased possibly because of competition of these transfer ligands with tricine. It was primarily to remove ^{99m}Tc colloids that the labeled RGD (Figure 3a) and labeled RGE (data not shown) were purified by SE HPLC before use. The purified ^{99m}Tc peptides were reanalyzed by RP HPLC, which showed a major sharp peak at 15.4 min in the radiochromatograms identical to that of the unpurified sample. This indicated that the major peak on both RP and SE HPLC was due to the desired ^{99m}Tc complexes.

The radiochemical purity, recovery, and the percentage of ^{99m}Tc colloid remained unchanged on standing for the unpurified labeled peptides over 20 h. After the HPLC purification, the radiochemical purity and recovery of both labeled RGD/E were over 95% by RP HPLC with or without 0.1% TFA in the mobile phase. Reanalysis by SE HPLC showed a single peak in both cases with a retention time of 23 min and recovery of 78−85% (Figure 3b). This indicated that the ^{99m}Tc-labeled peptides are stable in either acidic or neutral media (e.g. water or 0.1 M pH 7.2 PB).

High Specific Activity Preparation of Labeled RGD/E. High specific radioactivity could be achieved by labeling as little as 0.4 pmol to 4.3 nmol of both peptides with a large excess of ^{99m}Tc. The minimum molarity providing adequate radiolabeling by RP HPLC was about 4.3 pmol (5 ng), and in this case the labeling efficiency was only 10%. Labeling of higher amounts of peptide generally resulted in higher radiochemical yield, but the radiochemical recovery from RP HPLC remained unchanged (52−55%) due to ^{99m}Tc colloid formation. To optimize specific radioactivity, especially for cell binding studies, labeling of 43 pmol (50 ng) RGD/E with increasing amounts of ^{99m}Tc was investigated. The results, illustrated in Figure 4, show that the maximum specific radioactivity was approximately 20−30 Ci/μmol for both peptides (depending somewhat on the quality of ^{99m}Tc pertechnetate generator eluant). Therefore, in practice, 43 to 86 pmol (50 to 100 ng) of the peptide was labeled

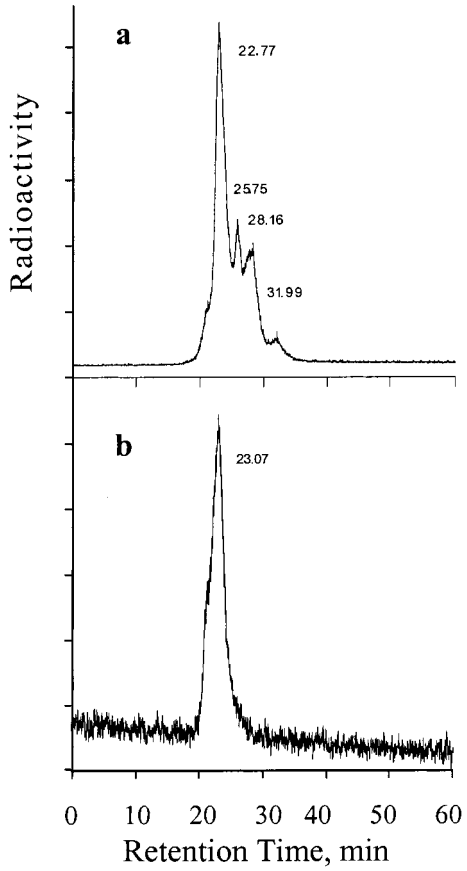

Figure 3. SE HPLC radiochromatograms of ^{99m}Tc-labeled-RGD before (panel a) and after the major peak was isolated and re-injected (panel b).

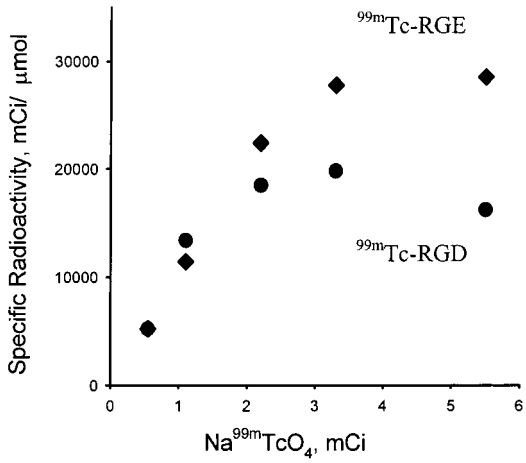

Figure 4. Influence on specific radioactivity of ^{99m}Tc-RGD (circles) or -RGE (squares) with increasing ^{99m}Tc radioactivity ranging from 0.5−5.5 mCi.

for both cell binding and animal studies. To ensure sufficient quantities of purified labeled peptides (100−300 μCi in 0.7 mL of phosphate buffer) for five animal injections, 86 to 129 pmol (0.1−0.15 μg) of peptide was used for each of the labelings.

Integrin Protein Binding. Figure 5 illustrates the UV chromatogram of 15 μg of $\alpha_V\beta_3$ integrin protein (top panel), the radiochromatograms of the mixture of 15 μg of integrin protein with 13 μCi of purified RGD (middle panel) or with 17 μCi of RGE (bottom panel). By comparison with labeled RGE, the ^{99m}Tc complex of RGD exhibited a shift with $\alpha_V\beta_3$ integrin protein on the chromatogram indicating specific binding. The binding

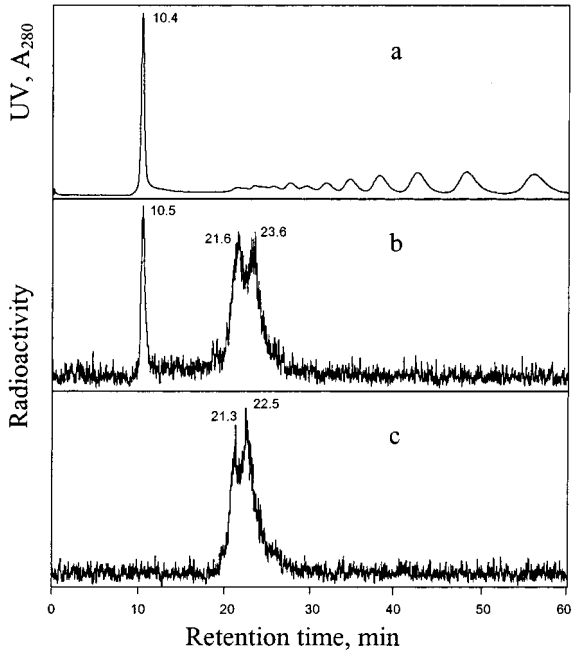

Figure 5. SE HPLC chromatograms of the $\alpha_V\beta_3$ integrin protein at 10.4 min in the UV (panel a) and the radioactivity profiles resulting from the addition to the $\alpha_V\beta_3$ integrin protein of ^{99m}Tc-RGD (panel b) and ^{99m}Tc-RGE (panel c) under similar conditions. A shift in the radioactivity profile to the retention time of the integrin is seen only in the case of RGD.

percentage of labeled RGD to $\alpha_V\beta_3$ integrin protein increased from 7.5% to 20.4% with a corresponding increase in the concentration of the integrin (0.2−0.5 μmol). By contrast, no significant binding was seen for labeled RGE. It is interesting that the majority of the label remained unbound even though the molarity of the integrin used was greater than the sum of the labeled and unlabeled RGD. This implies a weak association constant of RGD−HYNIC with the integrin. It may be assumed that one molecule of RGD binds with one integrin, and the binding equilibrium can be described by eq 1:

$$^{99m}\text{Tc-RGD} + \text{Integrin} = \text{Integrin} - (^{99m}\text{Tc-RGD}) \quad (1)$$

Then, if K is the equilibrium constant, eq 1 can be rewritten as eq 2:

$$\log\{[^{99m}\text{Tc-RGD}]_b/[^{99m}\text{Tc-RGD}]_f\} = \log K + \log[\text{Integrin}]_f \quad (2)$$

where $[^{99m}\text{Tc-RGD}]_b$ and $[^{99m}\text{Tc-RGD}]_f$ are the concentrations of the bound and the free ^{99m}Tc-RGD, respectively, while $[\text{Integrin}]_f$ is the concentration of the free $\alpha_V\beta_3$ integrin protein. The $[\text{Integrin}]_f$ was estimated from the difference of the total integrin used minus the integrin bound. Assuming that the labels, free or bound, and the unlabeled RGD were not decomposed when passing through the SE HPLC, the association constant K (eq 2) can be estimated from a log−log plot of the ratio of bound to free ^{99m}Tc-RGD, as detected by SE HPLC, vs the concentration of the free integrin. The plot (data not shown) exhibited a straight line with a slope of 1.17 (correlation coefficient $r = 0.98$) and an intercept of 6.8. The slope suggested that roughly one RGD was bound to each integrin protein, whereas the intercept indicated that the association constant of ^{99m}Tc-RGD−HYNIC with $\alpha_V\beta_3$ integrin protein was modest ($\sim 7 \times 10^6$ M^{-1}).

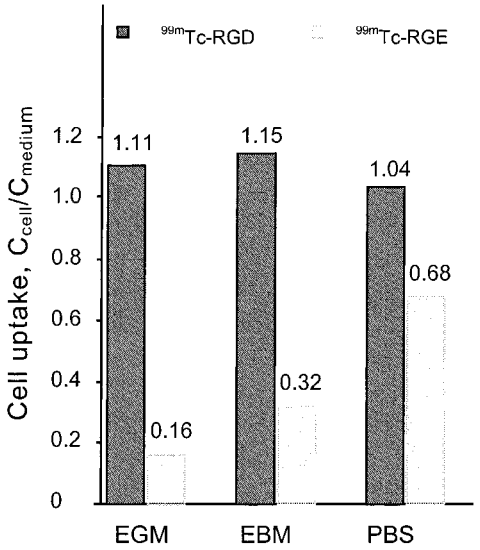

Figure 6. Histograms showing the ratio of counts in the pellet to counts in the supernatant i.e., C_{cell}/C_{medium}) for ^{99m}Tc-RGD and ^{99m}Tc-RGE added to HUVE cell incubated in three different media.

Table 1. The Relationship of the HUVE Cell Binding Ratios with the Specific Radioactivity of the Labeled RGD and RGE[a]

^{99m}Tc-RGD−HYNIC		^{99m}Tc-RGE−HYNIC		
specific activity, mCi/μmol	C_{cell}/C_{medium}	specific activity, mCi/μmol	C_{cell}/C_{medium}	cell uptake differentials, RGD/RGE
54	0.73	44	0.047	16
122	0.46	85	0.081	5.7
11000	1.11	17000	0.16	6.9
18000	1.38	35000	0.26	5.3

[a] The RGD and RGE radiolabels were purified by SE HPLC before use.

Cell Binding. SE HPLC purified labeled RGD/E were used as positive and control for HUVE cells binding, respectively. The results revealed that the ^{99m}Tc complexes exhibited important differences in cell binding as expected. For example, labeled RGD showed 5- to 16-fold higher binding than that of the control (Table 1). Cell uptake of both ^{99m}Tc complexes improved slightly when the specific radioactivity increased. However, this improvement in C_{cell}/C_{medium} was surprisingly small in comparison to the large change in specific radioactivity. Furthermore, the type of media influenced the binding of ^{99m}Tc-RGE but not ^{99m}Tc-RGD. The C_{cell}/C_{medium} ratios of ^{99m}Tc-RGD in HUVE cells in the three media were similar, while those of ^{99m}Tc-RGE varied with the media (Figure 6).

It was important in this research to estimate the average number of $\alpha_V\beta_3$ integrin expressed per cell since this value is a direct determinant of the potential of tumor imaging with ^{99m}Tc-labeled RGD. Scatchard plot is a common method used in determining the number of binding sites per cell by using ^{125}I-labeled macro molecules (*39*). However, an excessive molarity of peptide is usually required for the labeling with ^{99m}Tc (the ratio can be 100:1 or larger), and thus the unlabeled peptide would compete with the label for $\alpha_V\beta_3$ integrin protein binding. For this reason, using Scatchard plots to determine the cell-binding site with ^{99m}Tc-labeled peptide was assumed to be inappropriate (*40*). However, it was advisable to test the dependence of cell uptake on the concentration of labeled RGD in the medium. After 30 min incubation

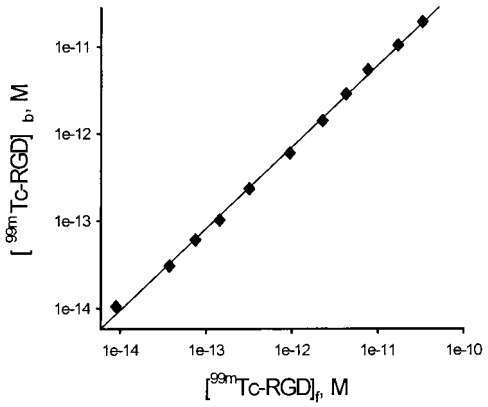

Figure 7. Log−log plot of concentration of ^{99m}Tc-RGD bound vs the complex present in supernatant. The subscript "b" stands for "bound" whereas "f" for "free".

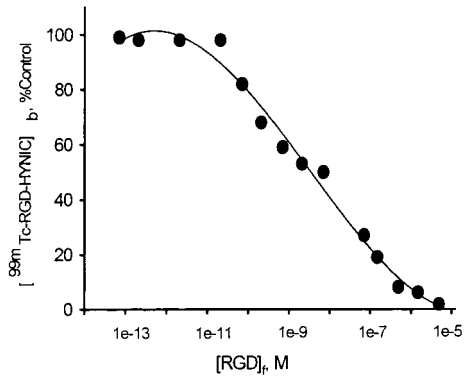

Figure 8. Semilog plot showing increasing inhibition of binding of purified ^{99m}Tc-RGD to HUVE cells with increasing concentrations of native RGD. Plotted as the percentage of bound ^{99m}Tc-RGD vs concentration of unlabeled RGD in supernatant. The subscript "b" stands for "bound" whereas "f" for "free".

with labeled RGD at temperatures close to 4 °C, the HUVE cells were isolated from the medium; the radioactivity in the cell pellets and in the supernatant was measured separately and expressed in terms of concentration (assuming 500 million HUVE cells have a volume of 1 mL). Figure 7 illustrates the log−log plot of concentration of the labeled RGD bound to HUVE cells vs that of the free drug in the medium. That a straight line with a slope of unity resulted suggested that the ^{99m}Tc-RGD was partitioned almost equally between cells and the medium. Accordingly, the uptake of labeled RGD in these cells under this experimental condition might not be generated from the binding with $\alpha_V\beta_3$ integrin protein but rather by a mechanism of passive diffusion or internalization. This diffusion might happen at the lowest concentration (10^{-14} M) of ^{99m}Tc-RGD tested. If this diffusion occurred after the saturation of the $\alpha_V\beta_3$ integrin by RGD, the number of binding sites on the cell must then be small and easily saturated.

Binding Competition Test. The above results show that $\alpha_V\beta_3$ binding sites on HUVC cells can be easily saturated. Since unlabeled RGD will compete with labeled RGD for a limited number of binding sites, a specific radioactivity as high as possible was necessary for the cell binding tests and for the animal imaging. After purification, 0.4 pmol of labeled RGD was added to 2.1×10^6 HUVE cells preincubated with increasing amounts of native RGD. Figure 8 shows the percent of labeled RGD bound vs the concentration of the native RGD added. The binding decreased with increasing

Table 2. Biodistribution of ^{99m}Tc-RGD and ^{99m}Tc-RGE in Nude Mice Bearing Xenotransplanted LS174T Tumors 6 h Postinjection[a]

	^{99m}Tc-RGD, $n = 2$		^{99m}Tc-RGE, $n = 2$	
organs	% ID/g	range	% ID/g	range
liver	2.00	0	1.70	0.10
heart	0.85	0.05	0.55	0.05
kidney	3.25	0.05	2.80	0.40
lung	1.10	0	0.90	0.10
spleen	1.35	0.05	0.45	0.05
stomach	2.60	0.60	0.95	0.05
sm. intestine	1.35	0.15	0.85	0.15
lg. intestine	2.20	0.10	2.10	0
muscle	0.35	0.05	0.30	0
tumor	0.75	0.05	0.60	0
blood	0.95	0.05	1.05	0.05
tumor/muscle	2.2	0.2	2.0	0
tumor/blood	0.8	0	0.6	0

[a] Each mouse received either 24 μCi of purified ^{99m}Tc-RGD or 24 μCi of ^{99m}Tc-RGE for the tests.

Table 3. Biodistributions of ^{99m}Tc-RGD−HYNIC and ^{99m}Tc-RGE−HYNIC in Nude Mice Bearing Xenotransplanted ACHN Tumors 6 h Postinjection[a]

	^{99m}Tc-RGD, (n=5)		^{99m}Tc-RGE, (n=5)		
organs	% ID/g	±SD	% ID/g	±SD	P values
liver	0.89	0.25	1.1	0.21	0.08
heart	0.45	0.06	0.51	0.15	0.20
kidney	3.5	0.96	4.6	0.83	0.04
lung	0.72	0.19	1.0	0.28	0.03
spleen	0.80	0.10	0.48	0.12	0.001
stomach	0.89	0.42	1.1	0.36	0.26
sm. intestine	1.0	0.37	0.44	0.07	0.005
lg. intestine	1.9	0.76	1.6	0.29	0.23
muscle	0.23	0.05	0.24	0.05	0.41
tumor	0.59	0.10	0.60	0.02	0.40
blood	0.36	0.06	1.1	0.25	0.0001
tumor/muscle	2.6	0.33	2.5	0.8	
tumor/blood	1.6	0.20	0.5	0.2	

[a] Each mouse received either 24 μCi of purified ^{99m}Tc−RGD or 24 μCi of ^{99m}Tc−RGE for the tests.

concentration of native RGD as expected with 50% binding blocked by approximately 7×10^{-9} M of native RGD.

In Vivo Animal Tests. Both LS174T and ACHN tumors were used for in vivo studies. While approximately the same radioactivity (24 μCi) was injected in each animal, each LS174T animal received 170 ng of labeled RGD/E while each ACHN animal received only 4.7 ng of these peptides. Images were taken 3 and 6 h postinjection. The biodistribution results at 6 h are listed in Table 2 (LS174T tumor) and in Table 3 (ACHN tumor). The accumulation in both tumors for both peptides was similar at 0.6−0.8% ID/g. Thus, the higher specific radioactivity used in the ACHN mice did not result in improved accumulations over that used in the LS174T mice.

DISCUSSION

Current methods of detecting cancer have both low specificity and sensitivity. There is, therefore, a pressing need for a widely available, noninvasive test for the diagnosis of cancer. It is likely that further gains in specificity and sensitivity can be achieved by using receptor-based imaging agents that target specific features of cancer tissue such as its neovasculature. In all neoplastic diseases, tumor growth and metastasis require persistent new blood vessels without which tumor cells become necrotic or apoptotic (41−45). Among the molecular markers associated with neovascular angiogenesis is the $\alpha_V\beta_3$ integrin, a protein that is absent or barely detectable in established blood vessels but is concentrated in forming blood vessels (*46*). Thus, the early and highly selective appearance of this integrin in tumor makes it a useful target for tumors imaging.

The cysteine-rich (*47*) cyclic polypeptide RGD-4C molecules were designed as $\alpha_V\beta_3$ integrin specific marker for tumor angiogenesis imaging. However, as reported (*33*), the number of $\alpha_V\beta_3$ integrin proteins expressed on endothelia or tumor cells may be limited. If the number of target integrins is limited, then a high specific radioactivity will be required to prevent saturation of integrin binding during imaging. Technetium may be complexed by ligands attached to biological molecules; however, thermodynamically, excessive chelator has to be applied for adequate chelation of ^{99m}Tc. It is thus difficult to achieve high specific radioactivity although there are examples. A unique method has been reported by Baidoo et al. (*48*). After the radiolabeling of a peptide containing a diaminedithiol chelator, the unlabeled peptide was removed on a iodoacetamide-derivatized gel resulting in a specific radioactivity of at least 100 Ci/μmol (the remaining unlabeled peptide was below the UV detection limit). Another successful approach to achieving high specific activity of ^{99m}Tc-labeled peptides used HYNIC as chelator and was reported by Liu et al. (*49*). A specific radioactivity of 20 Ci/mol was achieved by labeling 4.7 nmol of HYNICtide with 100 mCi of pertechnetate.

The coupling of NHS−HYNIC to RGD and RGE was convenient (*50*), and the purification of RGD−HYNIC and RGE−HYNIC by C18 Sep-Pak cartridge was simple and reproducible. Only 43−129 pmol of RGD/E (about 1% to 0.1% the amount of peptides usually used for ^{99m}Tc labeling) was successfully labeled in this laboratory at a specific radioactivity of approximately 20−30 Ci/μmol (the free RGD/E in the labeling solution was undetectable by UV) and therefore similar to the highest values reported by others (*48*, *49*). Despite the unavoidable formation of ^{99m}Tc colloids, a radiochemically pure ^{99m}Tc complex was produced as shown by a single major peak on RP and SE HPLC. When combined with SE HPLC purification, the purity and specific activity of the ^{99m}Tc-labeled peptide was suitable for cell binding and in vivo animal imaging.

The major radioactivity peak shown on both RP and SE HPLC was believed to be the desired complex for several reasons. First, the ^{99m}Tc labeling of the coupled RGD/E always showed the same single sharp peaks on RP HPLC radiochromatograms. Second, the retention times of the ^{99m}Tc-labeled RGD/E peptides on RP HPLC were always greater than those of the unlabeled peptides, indicating the labels were more lipophilic. Third, the nonspecific ^{99m}Tc-labeled RGD and RGE showed broad peaks and a lower labeling efficiency on RP HPLC and were unstable in acidic solvents, whereas the ^{99m}Tc complexes were stable either in acidic or neutral solvents.

The labeled RGD/E were purified by SE HPLC with 0.1 M pH 7.2 PB as eluant. The purity and stability of the purified ^{99m}Tc complexes were tested by reinjection to RP and SE HPLC. The results confirmed that the major peaks in both systems were due to the same complexes, that the purification was successful and reproducible, and that the complexes were stable in either acidic solution and phosphate buffer and therefore probably stable in cell binding and in vivo animal tests.

The uptake percentage of the labeled RGE to HUVE cells was always smaller than that of the labeled RGD

almost certainly because the former does not specifically bind to the $\alpha_V\beta_3$ integrin.

The ^{99m}Tc complexes of RGD/E also showed the expected differences in $\alpha_V\beta_3$ integrin protein binding. The binding percentage of the labeled RGD rose from 7.5% to 20.4% when the concentration of the integrin increased from 0.2 to 0.5 μM while no significant increase was detected in the case of labeled RGE. This indicates a specific association of labeled RGD but not RGE with the $\alpha_V\beta_3$ integrin. That the percentage shift on SE HPLC of the labeled RGD by the addition of a molar excess of the $\alpha_V\beta_3$ integrin protein (the molar ratios of the integrin protein to the total labeled and unlabeled RGD/E peptides were 14−18) is small may be due to the weak association constant (7×10^6 M^{-1}) since the manufacturer of the integrin protein guarantees the absence of significant contamination of the integrin with matrix binding proteins.

It was seen that the binding difference of ^{99m}Tc complexes on the $\alpha_V\beta_3$ integrin protein was consistent with that seen in the HUVE cell binding tests. The data in Table 1 show a slight increase in cell binding of the labeled RGD with a large increase in the specific radioactivity, suggesting the number of the specific binding sites may be small and saturation could occur even at this low concentration of RGD peptide. The binding of antigen−antibody or receptor−ligand normally shows an increase with dosage until saturating concentrations are reached (*51*−*53*). However, the straight line of Figure 7 implies nonspecific binding even when 3×10^6 cells were incubated with lowest concentration of labeled RGD. At that point, approximately 1.7×10^7 labeled RGD molecules (3×10^{-14} M) along with 3×10^9 molecules (4.8×10^{-12} M) of unlabeled RGD were incubated with 3 million cells. If this is the case, the upper limit of the concentration of the $\alpha_V\beta_3$ integrin may be by calculation as small as 4.8×10^{-12} M. This corresponds to only one $\alpha_V\beta_3$ protein expressed on each HUVE cell. A limited $\alpha_V\beta_3$ integrin expression on HUVE (*34*, *35*, *16*) and ACHN (*54*) cell types has been confirmed but not quantified.

Taken together, the labeled RGD peptides may have limited utility as markers for tumor imaging because the binding constant of ^{99m}Tc-RGD−HYNIC to the integrin is modest (7×10^6 M^{-1}) and because of the small number of the $\alpha_V\beta_3$ integrins expressed on each tumor cell. For example the concentration of labeled RGD specifically bound to the $\alpha_V\beta_3$ integrin may be estimated: when 20 μCi purified labeled RGD ($\sim 4 \times 10^{-14}$ mol, 2.8×10^{-11} M) is injected into a mouse with a 0.2 mL xenotransplanted tumor (approximately 10^8 tumor cells) and with a blood volume of approximately 1.4 mL, it may be calculated that only one molecule of labeled RGD would get bound to 1000 tumor cells. Any accumulation exceeding this value would then be nonspecific. This assumption is in agreement with the results of our in vivo animal tests showing minimal tumor uptake of radioactivity. The fact that the tumor uptake of labeled RGE was similar to that of RGD (Tables 2 and 3) and that increasing the specific radioactivity of labeled RGD/E did not significantly improve the tumor accumulations in vivo is evidence that the uptake in endothelial or tumor cells was nonspecific.

As discussed above, the in vivo tumor uptake showed no significant difference for labeled RGD and RGE. This seemed very likely due to the small number of $\alpha_V\beta_3$ integrins expressed on either tumor capillary cells or on the tumor cells being limited and easily saturated. If this is the case, it could be difficult to use ^{99m}Tc-labeled RGD as the tumor imaging agent because the percentage of ^{99m}Tc-RGD complex bound would be extremely low with a weak association constant.

CONCLUSION

Despite the use of RGD labeled at high specific activity, the tumor uptake of ^{99m}Tc-RGD−HYNIC in $\alpha_V\beta_3$ positive tumors growing in nude mice was marginal. These results are therefore in agreement with other investigators attempting to image this receptor with cyclic RGD peptides (*28*). In this investigation, we were able to confirm that the poor imaging results are probably a result of limited numbers of these receptors on the tumor used in this investigation and probably other tumors as well.

ACKNOWLEDGMENT

We wish to thank Ms. Loretta Lee and Dr. Yumin Zhang for providing the cells used in this study. We are grateful to Dr. Bruce Line for suggesting RGE as a control peptide and for other helpful suggestions. We thank Dr. A. Mike Rauth (Ontario Cancer Institute, Toronto, ON) for kind advice and helpful suggestions to this paper. This research was funded in part by DOD grant DAMD17-00-1-03326.

LITERATURE CITED

(1) DePasquale, J. A. (1998) Cell matrix adhesions and localization of the vitronectin receptor in MCF-7 human mammary carcinoma cells. *Histochem. Cell Biol. 110* (5), 485−94.

(2) Germer, M., Kanse, S. M., Kirkegaard, T., Kjoller, L., Felding-Habermann, B., Goodman, S., and Preissner, K. T. (1998) Kinetic analysis of integrin-dependent cell adhesion on vitronectin−the inhibitory potential of plasminogen activator inhibitor-1 and RGD peptides. *Eur. J. Biochem. 253* (3), 669−74.

(3) Vartanian, R. K., and Weidner, N. (1994) Correlation of intratumoral endothelial cell proliferation with microvessel density (tumor angiogenesis) and tumor cell proliferation in breast carcinoma. *Am. J. Pathol. 144* (6), 1188−94.

(4) Weidner, N. (1999) Tumour vascularity and proliferation: clear evidence of a close relationship. *J. Pathol. 189* (3), 297−9.

(5) Li, C., Guo, B., Bernabeu, C., and Kumar, S. (2001) Angiogenesis in breast cancer: The role of transforming growth factor beta and CD105. *Microsc. Res. Tech. 52* (4), 437−49.

(6) Zheng, D. Q., Woodard, A. S., Fornaro, M., Tallini, G., and Languino, L. R. (1999) Prostatic carcinoma cell migration via alpha(v)beta3 integrin is modulated by a focal adhesion kinase pathway. *Cancer Res. 59*(7), 1655−64.

(7) Felding-Habermann, B., O'Toole, T. E., Smith, J. W., Fransvea, E., Ruggeri, Z. M., Ginsberg, M. H., Hughes, P. E., Pampori, N., Shattil, S. J., Saven, A., Mueller, B. M. (2001) Integrin activation controls metastasis in human breast cancer. *Proc. Natl. Acad. Sci. U. S. A. 98* (4), 1853−8.

(8) Wong, N. C., Mueller, B. M., Barbas, C. F., Ruminski, P., Quaranta, V., Lin, E. C., Smith, J. W. (1998) Alpha(V) integrins mediate adhesion and migration of breast carcinoma cell lines. *Clin. Exp. Metastasis 16* (1), 50−61.

(9) Petitclerc, E., Stromblad, S., von Schalscha, T. L., Mitjans, F., Piulats, J., Montgomery, A. M., Cheresh, D. A., and Brooks, P. C. (1999) Integrin alpha(v)beta3 promotes M21 melanoma growth in human skin by regulating tumor cell survival. *Cancer Res. 59* (11), 2724−30.

(10) van der Zee, R., Murohara, T., Passeri, J., Kearney, M., Cheresh, D. A., and Isner, J. M. (1998) Reduced intimal thickening following alpha(v)beta3 blockade is associated with smooth muscle cell apoptosis. *Cell Adhes. Commun. 6*(5), 371−9.

(11) Chen, X., Wang, J., Fu, B., and Yu, L. (1997) RGD-containing peptides trigger apoptosis in glomerular mesangial cells of adult human kidneys. *Biochem. Biophys. Res. Commun. 234* (3), 594−9.

(12) Natali, P. G., Hamby, C. V., Felding-Habermann, B., Liang, B., Nicotra, M. R., Di Filippo, F., Giannarelli, D., Temponi, M., and Ferrone, S. (1997) Clinical significance of alpha(v)-beta3 integrin and intercellular adhesion molecule-1 expression in cutaneous malignant melanoma lesions. *Cancer Res. 57* (8), 1554−60.

(13) Hendrix, M. J., Seftor, E. A., Kirschmann, D. A., and Seftor, R. E. (2000) Molecular biology of breast cancer metastasis Molecular expression of vascular markers by aggressive breast cancer cells. *Breast Cancer Res. 2* (6), 417−22.

(14) Goligorsky, M. S., Noiri, E., Kessler, H., and Romanov, V. (1998) Therapeutic effect of arginine-glycine-aspartic acid peptides in acute renal injury. *Clin. Exp. Pharmacol. Physiol. 25* (3−4), 276−9.

(15) Sheu, J. R., Yen, M. H., Kan, Y. C., Hung, W. C., Chang, P. T., and Luk, H. N. (1997) Inhibition of angiogenesis in vitro and in vivo: comparison of the relative activities of triflavin, an Arg-Gly-Asp-containing peptide and anti-alpha(v)beta3 integrin monoclonal antibody. *Biochim. Biophys. Acta. 1336* (3), 445−54.

(16) Gawaz, M., Neumann, F. J., Dickfeld, T., Reininger, A., Adelsberger, H., Gebhardt, A., and Schomig, A. (1997) Vitronectin receptor (alpha(v)beta3) mediates platelet adhesion to the luminal aspect of endothelial cells: implications for reperfusion in acute myocardial infarction. *Circulation 96* (6), 1809−18.

(17) Tennant, T. R., Rinker-Schaeffer, C. W., and Stadler, W. M. (2000) Angiogenesis inhibitors. *Curr. Oncol. Rep. 2* (1), 11−6.

(18) Koyama, T., Nakajima, Y., Miura, K., Yamazaki, M., Shinozaki, M., Kumagai, T., and Sakaniwa, M. (1997) Analysis of extracellular matrix proteins in malignant chicken cell lines. *J. Vet. Med. Sci. 59* (5), 405−8.

(19) Maheshwari, G., Brown, G., Lauffenburger, D. A., Wells, A., Griffith, L. G. (2000) Cell adhesion and motility depend on nanoscale RGD clustering. *J. Cell Sci. 113* (Pt 10), 1677−86.

(20) Brooks, P. C., Montgomery, A. M., Rosenfeld, M., Reisfeld, R. A., Hu, T., Klier, G., and Cheresh, D. A. (1994) Integrin alpha v beta 3 antagonists promote tumor regression by inducing apoptosis of angiogenic blood vessels. *Cell 79* (7), 1157−64.

(21) Kang, I. C., Lee, Y. D., and Kim, D. S. (1999) A novel disintegrin salmosin inhibits tumor angiogenesis. *Cancer Res. 59* (15), 3754−60.

(22) Buckley, C. D., Pilling, D., Henriquez, N. V., Parsonage, G., Threlfall, K., Scheel-Toellner, D., Simmons, D. L., Akbar, A. N., Lord, J. M., and Salmon, M. (1999) RGD peptides induce apoptosis by direct caspase-3 activation. *Nature 397* (6719), 534−9.

(23) Ravi, D., Ramadas, K., Mathew, B. S., Panikkar, K. R., Nair, M. K., and Pillai, M. R. (2001) Apoptosis, angiogenesis and proliferation: trifunctional measure of tumour response to radiotherapy for oral cancer. *Oral Oncol. 37* (2), 164−71.

(24) Khalkhali, I., Villanueva-Meyer, J., Edell, S. L., Connolly, J. L., Schnitt, S. J., Baum, J. K., Houlihan, M. J., Jenkins, R. M., and Haber, S. B. (2000) Diagnostic accuracy of 99mTc-sestamibi breast imaging: multicenter trial results. *J. Nucl. Med. 41* (12), 1973−9.

(25) Arap, W., Pasqualini, R., and Ruoslahti (1998) Cancer treatment by targeted drug delivery to tumor vasculature in a mouse model. *Science 279*, 377−380.

(26) Pasqualini, R., Koivunen, E., and Ruoslahti (1997) α_V integrin as receptors for tumor targeting by circulating ligands. *Nature Biotech. 15*, 542−546.

(27) Haubner, R., Wester, H. J., Reuning, U., Senekowitsch-Schmidtke, R., Diefenbach, B., Kessler, H., Stocklin, G., and Schwaiger, M. (1999) Radiolabeled alpha(v)beta3 integrin antagonists: a new class of tracers for tumor targeting. *J. Nucl. Med. 40* (6), 1061−71.

(28) Haubner, R., Wester, H. J., Burkhart, F., Senekowitsch-Schmidtke, R., Weber, W., Goodman, S. L., Kessler, H., and Schwaiger, M. (2001) Glycosylated RGD-containing peptides: tracer for tumor targeting and angiogenesis imaging with improved biokinetics. *J. Nucl. Med. 42* (2), 326−36.

(29) Bogdanowich-Knipp, S. J., Jois, D. S., and Siahaan, T. J. (1999) The effect of conformation on the solution stability of linear vs cyclic RGD peptides. *J. Pept. Res. 53* (5), 523−9.

(30) Bogdanowich-Knipp, S. J., Chakrabarti, S., Williams, T. D., Dillman, R. K., and Siahaan, T. J. (1999) Solution stability of linear vs cyclic RGD peptides. *J. Pept. Res. 53* (5), 530−41.

(31) Koivunen, E., Wang, B., and Ruoslahti, E. (1995) Phage libraries displaying cyclic peptides with different ring sizes: ligand specificities of the RGD-directed integrins. *Biotechnology* (*NY*) *13* (3), 265−70.

(32) Ruoslahti, E. (1996) RGD and other recognition sequences for integrins. *Annu. Rev. Cell Dev. Biol. 12*, 697−715.

(33) van Hagen, P. M., Breeman, W. A., Bernard, H. F., Schaar, M., Mooij, C. M., Srinivasan, A., Schmidt, M. A., Krenning, E. P., and de Jong, M. (2000) Evaluation of a radiolabeled cyclic DTPA-RGD analogue for tumour imaging and radionuclide therapy. *Int. J. Cancer. 90* (4), 186−98.

(34) Kosugi, S., Tomiyama, Y., Honda, S., Kashiwagi, H., Shiraga, M., Tadokoro, S., Kiyoi, T., Kurata, Y., and Matsuzawa, Y. (2001) Anti-alphavbeta3 antibodies in chronic immune thrombocytopenic purpura. *Thromb. Haemost. 85* (1), 36−41.

(35) Pollman, M. J., Naumovski, L., and Gibbons, G. H. (1999) Vascular cell apoptosis: cell type-specific modulation by transforming growth factor-beta1 in endothelial cells versus smooth muscle cells. *Circulation 99* (15), 2019−26.

(36) Abrams, M. J., Juweid, M., TenKate, C. I., Schwartz, D. A., Hauser, M. A., Gaul, F. E., Fuccello, A. J., Rubin, R. H., Strauss, H. W., and Fischman, A. (1990) Technetium-99m-Human Polyclonal IgG Radiolabeled via the Hydrazino Nicotinamide Derivative for Imaging Focal Sites of Infection in Rats. *J. Nucl. Med. 31*, 2022−2028.

(37) Kosugi, S., Tomiyama, Y., Honda, S., Kashiwagi, H., Shiraga, M., Tadokoro, S., Kiyoi, T., Kurata, Y., and Matsuzawa, Y. (2001) Anti-alphavbeta3 antibodies in chronic immune thrombocytopenic purpura. *Thromb. Haemost. 85*(1), 36−41.

(38) Su, Z. F., Zhang, X., Ballinger, J. R., Rauth, A. M., Pollak, A., and Thornback, J. R. (1999) Synthesis and Evaluation of Two Technetium-99mTc-Labeled Peptidic 2-Nitroimidazoles for Imaging Hypoxia. *Bioconjugate Chem. 10*, 897−904.

(39) Renner, C., Stehle, I., Lee, F. T., Hall, C., Catimel, B., Nice, E. C., Mountain, A., Rigopoulos, A., Brechbiel, M. W., Pfreundschuh, M., and Scott, A. M. (2001) Targeting properties of an anti-CD16/anti-CD30 bispecific antibody in an in vivo system. *Cancer Immunol. Immunother. 50* (2), 102−8.

(40) Liu, S., and Edwards, D. S. (1999) ^{99m}Tc-Labeled Small Peptides as Diagnostic Radiopharmaceuticals. *Chem. Rev. 99* (9), 2235−2268.

(41) MacDonald, T. J., Taga, T., Shimada, H., Tabrizi, P., Zlokovic, B. V., Cheresh, D. A., and Laug, W. E. (2001) Preferential susceptibility of brain tumors to the antiangiogenic effects of an alpha(v) integrin antagonist. *Neurosurgery 48* (1), 151−7.

(42) Weidner, N. (1999) Tumour vascularity and proliferation: clear evidence of a close relationship. *J. Pathol. 189* (3), 297−9.

(43) Liu, W., Ahmad, S. A., Reinmuth, N., Shaheen, R. M., Jung, Y. D., Fan, F., and Ellis, L. M. (2000) Endothelial cell survival and apoptosis in the tumor vasculature. *Apoptosis 5* (4), 323−8.

(44) Kumar, C. C., Malkowski, M., Yin, Z., Tanghetti, E., Yaremko, B., Nechuta, T., Varner, J., Liu, M., Smith, E. M., Neustadt, B., Presta, M., and Armstrong, L. (2001) Inhibition of angiogenesis and tumor growth by SCH221153, a dual alpha(v)beta3 and alpha(v)beta5 integrin receptor antagonist. *Cancer Res. 61* (5), 2232−8.

(45) Pollman, M. J., Naumovski, L., and Gibbons, G. H. (1999) Endothelial cell apoptosis in capillary network remodeling. *J. Cell Physiol. 178* (3), 359−70.

(46) Brooks, P. C., Clark, R. A., and Cheresh, D. A. (1994) Requirement of vascular integrin alpha v beta 3 for angiogenesis. *Science 264* (5158), 569−71.

(47) Yeh, C. H., Peng, H. C., Yih, J. B., Huang, T. F. (1998) A new short chain RGD-containing disintegrin, accutin, inhibits

the common pathway of human platelet aggregation. *Biochim. Biophys. Acta 1425* (3), 493−504.

(48) Baidoo, K. E., Scheffel, U., Stathis, M., Finley, P., Lever, S. Z., Zhan, Y., and Wagner, H. N., Jr. (1998) High-affinity no-carrier-added 99mTc-labeled chemotactic peptides for studies of inflammation in vivo. *Bioconjugate Chem. 9* (2), 208−17.

(49) Liu, S., Edwards, D. S., Looby, R. J., Harris, A. R., Poirier, M. J., Barrett, J. A., Heminway, S. J., and Carroll, T. R. (1996) Labeling a hydrazino nicotinamide-modified cyclic IIb/IIIa receptor antagonist with 99mTc using aminocarboxylates as coligands. *Bioconjugate Chem. 7*(1), 63−71.

(50) Hnatowich, D. J., Chang, F., Lei, K., Qu, T., and Rusckowski, M. (1997) The influence of temperature and alkaline pH on the labeling of free and conjugated MAG3 with technetium-99m. *Appl. Radiat. Isot. 48* (5), 587−94.

(51) Hu, D. D., Hoyer, J. R., and Smith, J. W. (1995) Ca2+ suppresses cell adhesion to osteopontin by attenuating binding affinity for integrin alpha v beta 3. *J. Biol. Chem. 270* (17), 9917−25.

(52) Pelletier, A. J., Kunicki, T., and Quaranta, V. (1996) Activation of the integrin alpha v beta 3 involves a discrete cation-binding site that regulates conformation. *J. Biol. Chem. 271* (3), 1364−70.

(53) Kunicki, T. J., Annis, D. S., and Felding-Habermann, B. (1997) Molecular determinants of arg-gly asp ligand specificity for beta3 integrins. *J. Biol. Chem. 272* (7), 4103−7.

(54) Korhonen, M., Sariola, H., Gould, V. E., Kangas, L., and Virtanen, I. (1994) Integrins and laminins in human renal carcinoma cells and tumors grown in nude mice. *Cancer Res. 54* (16), 4532−8.

BC0155566